journal

Mullite Processing, Structure, and Properties

J. Am. Ceram. Soc., 74 [10] 2343–58 (1991)

Mullite for Structural, Electronic, and Optical Applications

Ilhan A. Aksay,* Daniel M. Dabbs,* and Mehmet Sarikaya*

Department of Materials Science and Engineering and Advanced Materials Technology Center, Washington Technology Center, University of Washington, Seattle, Washington 98195

Mullite ($3Al_2O_3 \cdot 2SiO_2$) is becoming increasingly important in electronic, optical, and high-temperature structural applications. This paper reviews the current state of mullite-related research at a fundamental level, within the framework of phase equilibria, crystal structure, synthesis, processing, and properties. Phase equilibria are discussed in terms of the problems associated with the nucleation kinetics of mullite and the large variations observed in the solid-solution range. The incongruent melting behavior of mullite is now widely accepted. Large variations in the solid solubility from 58 to 76 mol% alumina are related to the ordering/disordering of oxygen vacancies and are strongly coupled with the method of synthesis used to form mullite. Similarly, reaction sequences which lead to the formation of mullite upon heating depend on the spatial scale at which the components are mixed. Mixing at the atomic level is useful for low-temperature (<1000°C) synthesis of mullite but not for low-temperature sintering. In contrast, precursors that are segregated are better suited for low-temperature (1250° to 1500°C) densification through viscous deformation. Flexural strength and creep resistance at elevated temperatures are significantly affected by the presence of glassy boundary inclusions; in the absence of glassy inclusions, polycrystalline mullite retains >90% of its room-temperature strength to 1500°C and displays very high creep resistance. Because of its low dielectric constant, mullite has now emerged as a substrate material in high-performance packaging applications. Interest in optical applications mainly centers on its applicability as a window material within the mid-infrared range. [Key words: mullite, processing, substrates, infrared, transparent materials.]

I. Introduction

PHASES of the SiO_2–Al_2O_3 and the SiO_2–Al_2O_3–H_2O systems have had, and will continue to have, a significant role in the development of traditional and advanced ceramics. As hydrous aluminum silicates, clay-based minerals have been used since the shaping of the first manmade ceramic products.[1] Among the anhydrous forms, the group of sillimanite ($Al_2O_3 \cdot SiO_2$) minerals (sillimanite, kyanite, and andalusite) (the phases that form at high pressures) and mullite ($3Al_2O_3 \cdot 2SiO_2$) (the only stable phase under atmospheric conditions) are well-known for their importance in refractories. In addition to these traditional applications, mullite in particular has received significant attention during the last decade as a potential matrix material for high-temperature structural applications, principally because it retains a significant portion of its room-

S. M. Wiederhorn—contributing editor

Manuscript No. 196458. Received August 19, 1991; approved September 3, 1991.

Supported by the U.S. Air Force Office of Scientific Research under Grant No. AFOSR-91-0040 and the Department of Energy, Office of Basic Sciences, under Contract No. 063961-A-F1.

*Member, American Ceramic Society.

temperature strength at elevated temperatures and displays very high creep and thermal-shock resistance.[2-4] Furthermore, mullite is now used as a ceramic substrate in multilayer packaging[5] and has been shown to be a strong candidate as a window material in the mid-infrared range.[6]

Although it is one of the most commonly found phases in industrial ceramics, the importance of mullite as a ceramic phase was only recognized during this century in the pioneering work of Bowen and Grieg[7] published in 1924. This late recognition can be attributed to two factors: (i) the occurrence of mullite as a mineral is very rare in nature, and, (ii) although it is a very common reaction product of most aluminum silicates at high temperatures (>1000°C), mullite was mistakenly identified as a sillimanite mineral in some earlier studies.[8] Sillimanite and its two polymorphs have orthorhombic crystal structures very similar to that of mullite, but at atmospheric pressure the sillimanite minerals always convert to mullite at elevated temperatures.[9] The mullite compound, $3Al_2O_3 \cdot 2SiO_2$, is named after the Isle of Mull in the northern highlands of Scotland, where a rare occurrence of this compound is found in nature (Fig. 1).[7] The occurrence of this compound on the Isle of Mull is thought to be a result of post-Caledonian volcanic activities in which clay mineral deposits, heated through contact with magma, produced a high-temperature mullite phase.[11]

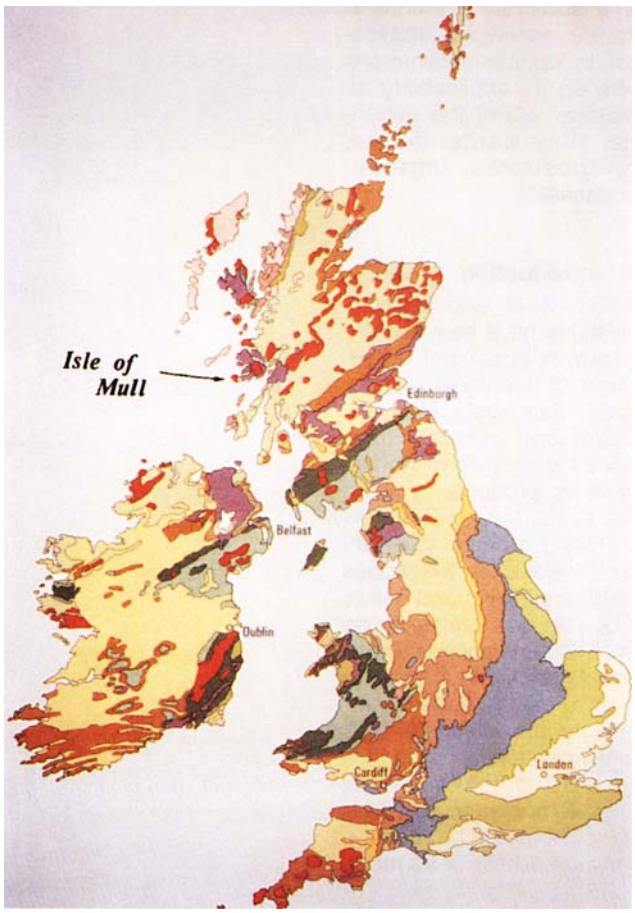

Fig. 1. Geological map of Britain and Ireland showing the location of sedimentary and igneous rocks with the color code of the international scale for geological maps. Igneous rocks are coded with red and violet. The Isle of Mull in the northern highlands of Scotland is marked as a site of past volcanic activity. Because of a rare occurrence of the compound $3Al_2O_3 \cdot 2SiO_2$ on this island as a reaction product of clays, the compound was named "mullite."[11]

Scientific and technological developments as they relate to mullite can be categorized in three time periods. In the first period, from 1924 to 1950, the bulk of research activity was on the structural characterization of mullite with respect to the sillimanite group minerals. Most of the relevant studies from this period were well documented in an extensive review monogram by Grofcsik and Tamas.[12] In the second period, starting in 1950, publications by Bauer *et al.*[13,14] on the growth of the first single crystals of mullite by the Vernuil process raised doubts about the incongruent melting of mullite as reported by Bowen and Greig in 1924, and thus laid the pathway for a long series of phase equilibria studies on the SiO_2–Al_2O_3 system. The significant developments of this second period were reviewed by Davis and Pask.[15] Although the studies on phase equilibria are still of concern today, in the third period, starting in the mid-1970s, the emphasis clearly shifted to the development of mullite as an advanced ceramic for structural, optical, and electronic applications. The beginning of this third period appears to coincide with the use of mullite single crystals in a creep study at 1500°C that showed that, at stress levels up to 876 MPa, mullite did not deform plastically.[16]

Much of the progress in the third period was assessed at the international workshop on mullite held in Tokyo, Japan, in November 1987.[17] Because of rapid progress in the field, a follow-up symposium to this workshop was organized on "Mullite Processing, Structure, and Properties" during the American Ceramic Society Pacific Coast Regional Meeting held in Seattle, Washington, in October 1990.[18] Many of the papers presented at the Seattle symposium are now compiled as part of this special issue.

As a complement to the articles included in this issue, this feature article provides a broader perspective on the development of mullite for structural, optical, and electronic applications. Recognizing that further developments necessitate a thorough understanding of processing–structure–property relations, in the following sections we discuss the unresolved issues with respect to phase equilibria, structure, and the processing of mullite with the key ac-

complishments of the last decade. Next, the impact of these accomplishments on property control is illustrated with brief discussions on the mechanical, electronic, and optical properties of mullite-based ceramic systems.

II. Phase Equilibria

The key problems of phase equilibria in the SiO_2–Al_2O_3 system can be discussed in two categories: (i) the melting behavior of mullite and (ii) the solid-solution range of the mullite phase field.[6,19–23] Although uncertainties remain on the exact location of the immiscibility region, our discussion here is confined only to these two problems since they more directly relate to the control of the microstructural features of single-phase mullite systems. The first problem relates to the nucleation kinetics of mullite and/or alumina in aluminum silicate melts and is discussed in this section. The second problem, which requires an understanding of the crystal structure of mullite, is discussed in Section III. Since many of the details on these issues have been extensively covered in recent reviews,[24–26] our discussion is brief and focuses on what appear to be the reasons for the dilemma that has resulted in more than 70 years of confusion in the field.

The results of two recent noteworthy phase equilibria studies on the SiO_2–Al_2O_3 system are reproduced in Figs. 2(A) and 3.[20–23] Figure 2(A) summarizes the results from the work by Aksay and Pask,[20,21] and Fig. 3 is from the study by Klug *et al.*[22,23] At first glance, the main common feature of these diagrams is the incongruent melting behavior of mullite, which agrees with the original work of Bowen and Grieg. The main differences between the diagrams center on (i) the peritectic temperature and composition and (ii) the extent of the solid-solution range. These differences are quite significant and puzzling especially since both studies represent a set of very carefully performed experiments. When faced with this dilemma, the usual solution has been to assume that one of the diagrams is correct and the other is wrong. A proper approach, however, is first to assume that both sets of experimental results are correct but that the differences are in the interpretation of the results. Following this approach, in Fig. 2(B), we superimpose the latest version of the Klug *et al.*[22,23] phase diagram (Fig. 3) on the Aksay and Pask[21] diagram of Fig. 2(A). Note that the composite diagram of Fig. 2(B) reveals two other important points: (i) the metastable extension of the phase field in one diagram totally encompasses the stable phase field of the other, and (ii) the metastable (congruent) melting temperature of one perfectly matches the stable (incongruent) melting point of the other. The problem then reduces to trying to understand the conditions that led us to observe these differences and to differentiate between the stable and metastable states. By virtue of the unique diffusion couple technique used to determine the diagram in Fig. 2(A), it at present stands out as the one that provides a more unifying view of stable and metastable states.

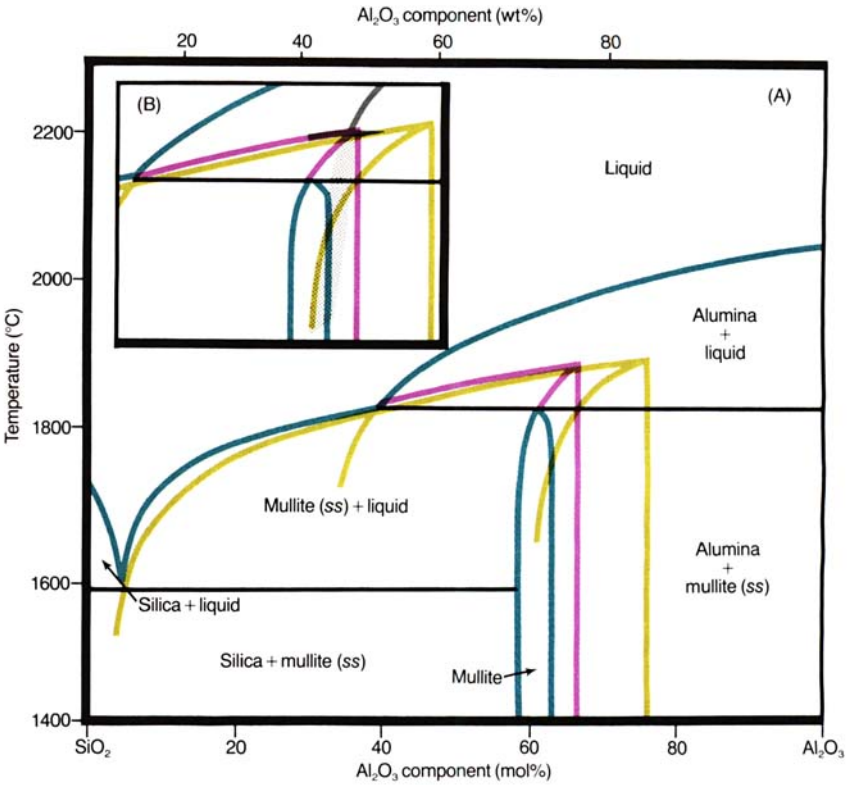

Fig. 2. (A) Stable and metastable phase diagram of the SiO_2–Al_2O_3 system, as determined by diffusion-couple experiments and through characterization of melt-quenched samples.[20,21] Insert in (B) superimposes the solid-solution range of mullite (shaded region) as determined by Klug *et al.*[22,23] on the diagram of (A).

The diffusion couple technique leading to the diagram in Fig. 2(A) is unique since it can be utilized to determine the stable *and* metastable equilibrium assemblages.[27] This point can be illustrated with an example that addresses the problem of nucleation in aluminum silicate melts and thus the consequential confusion on the exact location of the peritectic composition. Diffusion-zone microstructures of three diffusion couples, each of which was annealed at 1903°C for 15 min, but cooled at different rates, are shown in Fig. 4. These microstructures differ drastically, although the average composition profiles and the liquidus compositions at the alumina single-crystal interface—as obtained by scanning an electron beam over an area affected by localized crystallization—are identical. The precipitated crystalline phase, as determined by electron microprobe and X-ray diffraction (XRD) is mullite in the

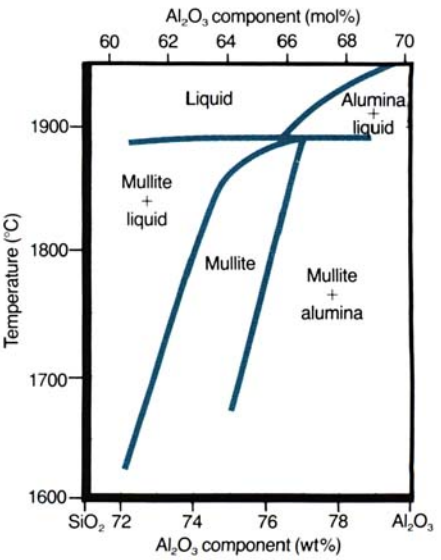

Fig. 3. SiO_2–Al_2O_3 phase diagram, as determined through microstructural characterization of quenched samples.[22,23] Note that when this diagram is superimposed on Fig. 2(A), the solid-solution range falls completely within the solid-solution range of ordered mullite (Fig. 2(B)).

couple that was quenched (Fig. 4(A)), alumina in the couple that was cooled relatively slowly (Fig. 4(C)), and a composite of alumina and mullite in the couple that was cooled at a moderate rate (Fig. 4(B)). Since the liquidus composition at the peritectic temperature is 52.3 wt% alumina, ~350 μm of the diffusion zone adjacent to the alumina portion of the diffusion couple would experience some alumina precipitation during equilibrium cooling (Fig. 2(A)). The absence of alumina in this portion of the diffusion zone of a quenched couple (Fig. 4(A)) and the presence of alumina in a slowly cooled couple (Fig. 4(C)) can be explained only on the basis of supercooling of the liquid. Therefore, note that, although the overall composition profiles obtained by averaging over an area are independent of the nature of the microstructure and always provide information on the stable equilibrium conditions, microstructural observations could yield conflicting results depending on the experimental conditions followed. Consequently, when a phase diagram is determined only by microstructural examination of quenched samples, either one of the phase diagrams may be proposed as the stable one since the microstructure of Fig. 4(A) would lead an investigator to propose the diagram of Fig. 3, whereas the microstructure of Fig. 4(C) would lead to Fig. 2(A). However, independent of the microstructural features, the composition profiles in all microstructures support Fig. 2(A) as the stable diagram although more work is needed to clearly understand the conditions that lead us to the metastable states.

III. Crystal Structure of Mullite

The crystal structure of mullite is a modified defect structure of sillimanite, $Al_2O_3 \cdot SiO_2$, in which the mullite stoichiometry is achieved by substituting Si^{4+} ions with Al^{3+} ions in the tetrahedral sites of the alternating aluminum and silicon columns, as in the scheme $2Si^{4+}+O^{2-}=2Al^{3+}+\square$ (Fig. 5).[28,29] The crystal structure is orthorhombic, and the average composition may range from $3Al_2O_3 \cdot 2SiO_2$ (3/2) to $3Al_2O_3 \cdot SiO_2$ (3/1).[19-21,30-34] This is achieved by the removal of oxygens from the O(3) positions (tetrahedral linking oxygens)[35] and by a readjustment of cations from the T to T^* type in partially occupied columns formed by linking $(Si, Al)O_4$ tetrahedra (Fig. 6).[28,31,33,35] The octahedral AlO_6 clusters (Fig. 5), which form the columnar structure by sharing edges, and the center of the orthorhombic unit cell do not change during this rearrangement. In general, the elemental composition of mullite in this well-accepted defect structure is expressed as

$$Al_2^{VI}(Al_{2+2x}^{IV}Si_{2-2x})O_{10-x}$$

where x denotes the amount of missing oxygen from the formula and VI and IV denote sixfold and fourfold coordinations of aluminum, respectively, and silicon occupies the fourfold positions. Although the ordering of aluminum on the sillimanite-type $(Al, Si)^{IV}$ sites cannot

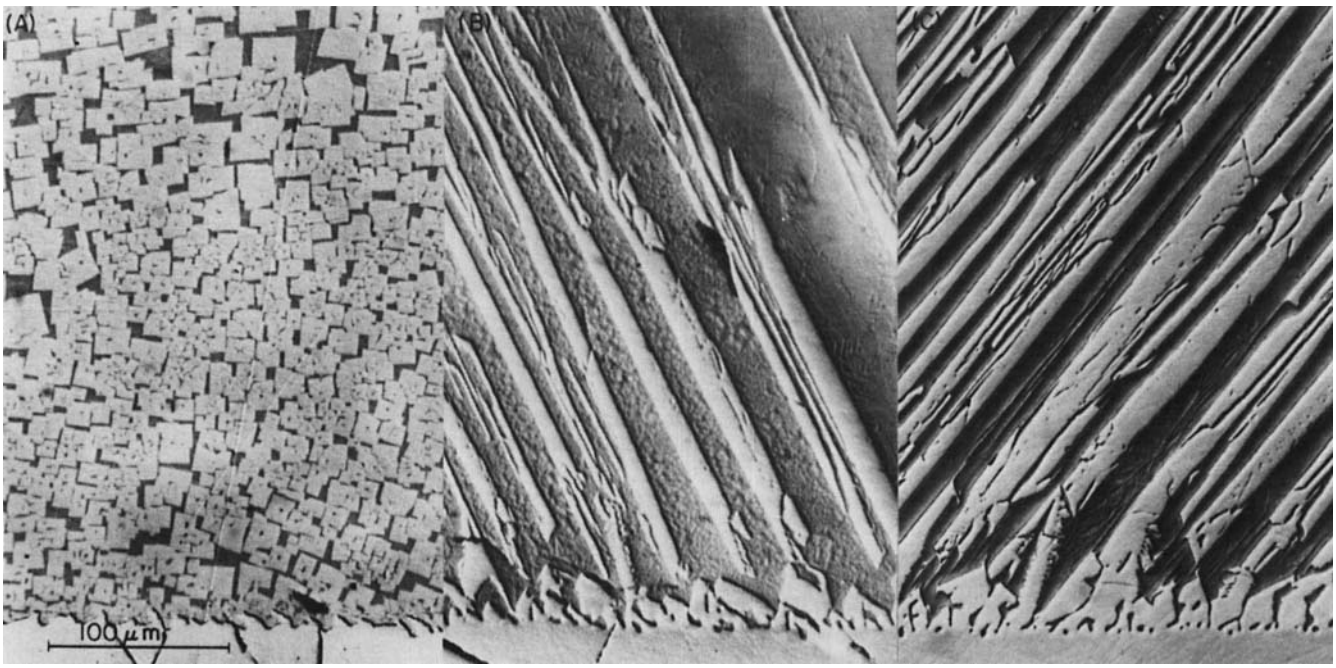

Fig. 4. Interference-contrast micrographs of the reaction zone between a diffusion couple of alumina single crystal (bottom) and fused silica (top) annealed at 1903°C for 900 s and quenched at different rates: (A) the fastest and (C) the slowest. Precipitates in the top portion of the diffusion zone are (A) mullite (light gray); (B)' alumina (light-gray needles) and mullite (fine precipitates between the alumina needles); and (C) alumina (light-gray needles). All three have identical concentration profiles.[21]

be detected, the new $(Al)^{VI}$ sites can be detected by XRD and electron diffraction analyses.[28,29,32,33,36,37] It has been observed that x continuously changes from 0.17 to 0.6 in parallel with the ordering of the vacancies on the O(3) site. For example, for $x=0.25$, the composition becomes $3Al_2O_3 \cdot 2SiO_2$ (space group *Pbam;* unit-cell dimensions $a=7.540$ Å, $b=7.680$ Å, and $c=2.885$ Å (1 Å $=10^{-1}$ nm)), and, for $x=0.57$, the composition is $3Al_2O_3 \cdot SiO_2$.

Structural studies, which have concentrated primarily on the effects of kinetics, temperature, and composition, in the presence or absence of alumina, have resulted in the development of various forms of mullite structures. All of these factors can promote the development of metastable forms of mullite because of ordering/disordering of oxygen vacancies.[33,35,38,39] The ordering phenomena in mullite have been studied by examining extra reflections that are produced in XRD and electron diffraction patterns.[28,29,32,33,36,37,40] These reflections are either in the form of satellite reflections (sharp and diffuse, denoted by S-mullite and D-mullite, respectively)[30] or in diffuse streaks in which sharpness indicates the ordering and diffuseness indicates the disordering. Generally, when mullite is synthesized from a melt of high alumina content and then quenched to room temperature, its structure is highly ordered and a pair of sharp reflections occur around the {*h*0*l*} reflections of the matrix; the sharpness changes with respect to the alumina content in the structure. The solid-solubility limit of alumina in mullite can extend as high as 83.2 wt% (76 mol%) when mullite is formed from a melt.[21,41] In these aluminous concentrations, the mullite lattice is heavily twinned, with twin spacing in the nanometer range.[42] In this case, depending on the initial concentration of alumina and the cooling procedures, a continuous change in the composition of mullite can be obtained from an alumina/silica ratio of 1.5 to 3.17.[21,33]

On the other hand, the stable form of mullite has the 3/2 composition of alumina and silica when mullite is formed from diffusion couples of silica and alumina.[21] In these cases, the mullite lattice is highly disordered and is fairly uniform without twinning or other ordering-induced defects. High-resolution electron microscopy (HREM) images taken from extremely thin areas (<20 Å) of a 3/2 mullite indicate the presence of oxygen vacancies along the O(3)-type columns.[43] These images also indicate at least 50% cation displacement from the nearest neighbors to *T*- and *T**-type columns. This displacement is presumably a result of vacancies created in oxygen sites, which are randomly distributed (and thus

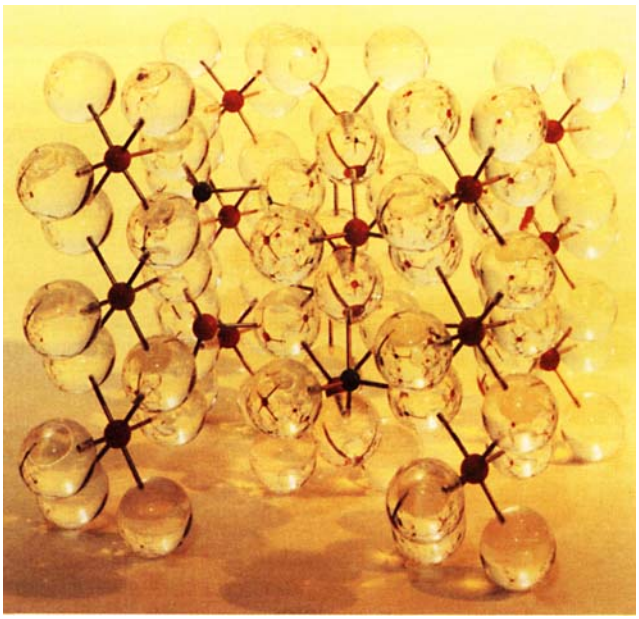

Fig. 5. Ball model of sillimanite ($Al_2O_3 \cdot SiO_2$) which serves as the basis of mullite unit cell. Large transparent balls represent oxygen ions, red balls represent sixfold and fourfold coordinated aluminum ions, and green balls represent silicon atoms.

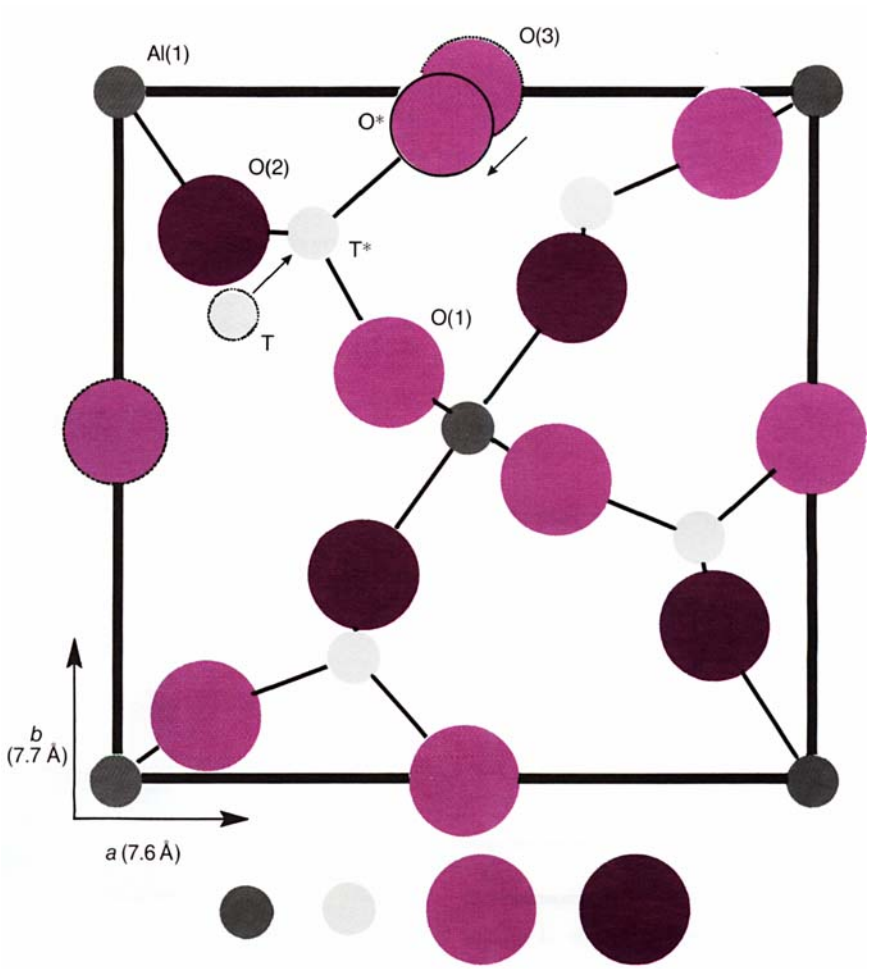

Fig. 6. Projection along [001] direction of the ideal unit cell of mullite showing *T* to *T** transition of the cations (indicated by an arrow) following the formation of oxygen vacancy (large dotted circle) and readjustment of oxygen in the O(3) positions.

these sites do not produce diffuse scattering in the electron diffraction patterns).

Structural analysis studies of various mullites formed using solid-state reactions or melt-grown samples indicate that mullite can have a solid-solubility range from about 70 to 84 wt% alumina ($x=0.17$ and $x=0.59$, respectively), which is consistent with the phase equilibria studies.[6,21,32] The issue of alumina solubility is still disputed in these studies, especially with respect to the extent of the solubility range near the peritectic transformation. However, despite numerous structural studies, there has been no systematic study to determine the exact conditions under which these ordered and disordered structures form and the nature of their compositions. For example, it is very probable that several different forms of mullite are present in a given sample prepared under a set of synthesis conditions involving differential heating and cooling, which may cause changes in the heterogeneous distribution of diffusing species (e.g., oxygen) and, hence, result in nonuniform ordering. Therefore, it would be useful if future studies were directed toward the determination of the precise limits of sub-phase fields of various mullite compositions prepared under controlled kinetic and thermodynamic conditions. These studies would, then, identify whether it is possible to have several forms of mullite, both ordered and disordered, at a given temperature but with slightly different compositions and the phase transformation conditions of these structures. These studies would be essential for identifying these structures and their phase stabilities and other physical properties.

IV. Synthesis and Processing

Driven by the need to produce high-quality mullite for optical, dielectric, and structural applications, progress in the last decade on the synthesis and processing of mullite has been exemplary.[6,17,44,62] With the use of chemically synthesized powders and colloidal consolidation methods, it is now possible to produce almost single-phase mullite in the temperature range of 1250° to 1500°C (Fig. 7).[45,48,50,53,59,62] In comparison to conventional methods that require either hot-pressing above 1500°C or pressureless sintering above 1650°C, low-temperature-processing methods allow pressureless sintering of mullite-matrix composites,[59] cosintering with metals in multilayer packaging,[5] and fiber processing (Fig. 8).[63]

Since nature has not been generous in providing us with minerals that contain a moleculary mixed state of aluminum and silicon at the stoichiometric composition of mullite, until recent years most commercial products were produced through reaction sintering of mixed minerals (e.g., clays with alumina).[47] In such systems, the scale of chemical homogeneity is limited to the size of the particles, and, thus, global homogenization to the mullite stoichiometry is left to the high-temperature (>1650°C) heat-treatment stage.[47]

Today, high-quality commercial powders of mullite are produced by nanometer-scale mixing of aluminum, silicon, and oxygen. A recent extensive review by Sacks *et al.*[64] provides detailed information on the various

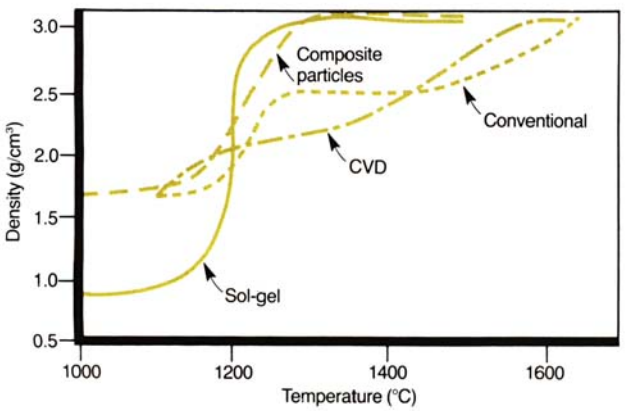

Fig. 7. Densification behavior of mullite is compared among samples prepared by a diphasic sol–gel route,[48] colloidal mixing of α-alumina and kaolinite (conventional),[48] colloidal consolidation of composite powders,[62] and CVD-processed powders.[53,58] Low-temperature sintering of sol–gel and composite-processed powder systems is due to viscous deformation of amorphous silica-rich matrix.

Fig. 8. Mullite fibers are used in thermal and electrical insulation, reinforcement, and high-temperature filtration. Another application is in fire-resistant fabrics to protect booms that are used to collect oil spilled on water. As shown in this figure, using a composite fabric containing NEXTEL 440 ceramic fibers of 3M Co. (3M Fire Boom), the oil may be burned in situ under controlled conditions when retrieval is not possible or practical. High-temperature properties of the fabric allow the boom to maintain an effective oil barrier after exposure to a long, intense oil fire.

methods used in the preparation of mullite-based powders. Many of the articles included in this issue also address the methods used to synthesize and process mullite through molecular and colloidal routes. The key concepts that have emerged from these recent studies are summarized below.

(1) Low-Temperature (<1250°C) Reaction Pathways to Mullite

The reaction sequences of molecularly and/or colloidally prepared mullite-forming precursors show strong resemblances to those observed in clay-based systems.[65-69] When the scale of chemical homogeneity is at the atomic level (i.e., monophasic precursors), mullite formation is typically observed at ~980°C through an exothermic reaction.[66-69] For instance, amorphous powders produced by chemical vapor deposition (CVD) or spray pyrolysis directly transform to mullite.[66,70,71] Similarly, slow hydrolysis of mixed alkoxide or salt-solution constituents can retain a finer scale of mixing between the two components and thus promote mullite formation directly.[49,52,66,72]

In contrast, when the scale of homogeneity is in the nanometer range (~1 to 100 nm) (i.e., diphasic precursors), mullite formation is generally preceded by the formation of transient alumina phases and can be delayed to temperatures as high as 1300°C, as evidenced by a second exothermic reaction at >1200°C.[45,50,55-57,69] For instance, powders or gels that are prepared through rapid hydrolysis of salt or alkoxide solutions yield diphasic-type precursors.[45,51,72,73] Coincidentally, in these systems, the cubic alumina (spinel) phase that is usually observed as the transient alumina also crystallizes through an exothermic reaction at ~980°C. The occurrence of mullite and/or the spinel phase almost at the same temperature then becomes the source of confusion in deciding which one of the phases is responsible for the 980°C reaction.

The reaction series of kaolinite ($2SiO_2 \cdot Al_2O_3 \cdot 2H_2O$) or metakaolinite ($2SiO_2 \cdot Al_2O_3$) is similar to that of diphasic precursors.[65,66] Initially, a γ-alumina-type spinel forms at 980°C.[68] Then, mullite crystallization follows at higher temperatures, often with a distinct second exotherm at ~1200°C. This similarity between the reaction series of kaolinite and diphasic precursors is important since it establishes a clear standard for the type of mixing that is required to convert a precursor directly to mullite. Although kaolinite is an atomically layered structure of $(Si_2O_5)^{2-}$ and $(Al_2(OH)_4)^{2+}$ molecular sheets, this level of mixing is still not sufficient to prevent the segregation of alumina and silica. In fact, there is evidence that further segregation takes place when metakaolinite goes through a spinodal-type coarsening prior to the 980°C crystallization.[68]

(2) Microstructure Evolution During (<1300°C) Heat Treatment

In the conventional approach, when mullite is produced through reaction sintering of alumina and silica at temperatures above 1650°C, the nucleation and growth of mullite occurs as an interfacial reaction product between alumina and silica.[20,21] In this case, the growth rate is controlled by the diffusion of aluminum and silicon through the mullite layer. Since this is a parabolic rate process, mullitization slows down with time, and, consequently, the elimination of the siliceous liquid phase becomes difficult with grain growth.

In the case of low-temperature (<1300°C) processing of mullite with diphasic precursors, however, a completely different mechanism than what is observed at high temperatures appears to control the nucleation and growth of mullite.[55,56,60,74] In diphasic systems, although alumina is present prior to the formation of mullite, the nucleation of mullite is not at the alumina–matrix interface but instead is within the siliceous amorphous matrix.[60,74] The apparent mechanism is the nucleation of mullite within the matrix as the matrix reaches the saturation concentration necessary to support mullite nucleation.[74] This nucleation is then the cause of the second exothermic reaction discussed above. Subsequent growth of mullite is controlled by the dissolution of alumina in the matrix but not by inter-

Corning's luminescent window made of Cr^{3+}-doped mullite glass-ceramic. Low dielectric constant and optical transparency of fine-grained polycrystalline mullite has led to interest in potential applications as a host material as a solid-state laser activator. In highly crystalline glass-ceramic, quantum efficiencies of 30% to 40% have been reported; in glass, quantum efficiencies are less than 1%; in single crystal, efficiencies are close to 100%.

diffusion through mullite. The transmission electron microscopy (TEM) study described below illustrates this point.

Figures 9(A) and (B) show characteristic regions of a sample prepared by colloidal mixing of α-alumina and high-purity kaolinite to attain an overall composition of $3Al_2O_3 \cdot 2SiO_2$ and then heat-treated to 1300°C for 1 h to achieve partial densification and mullitization. Note that mullite crystallites, 5 to 100 nm in size, are all found within the amorphous matrix, but none are observed in association with alumina particles. Many of the crystallites are already in contact with each other (Fig. 9(B)). A higher magnification image (Fig. 9(C)) of the interface region of the bicrystal shown in Fig. 9(B) reveals the lattice structures of both crystallites (the dark one in the [001] orientation and the other in the [123] orientation) and no amorphous region at the interface. The significance of this image is that glass-free interfaces between mullite grains start developing even at these early stages of mullite formation.[75]

Another significant observation is that mullite which forms in amorphous precursors at low temperatures (~1000°C) can have a tetragonal structure[76] with high alumina contents approaching 83 wt% (74 mol%).[32,66,73,76] This observation parallels the findings discussed in Sections II and III on high-alumina-content mullites that crystallize in melts quenched from high temperatures. However, when heated to temperatures higher than 1200°C, the alumina content decreases toward the stoichiometric (60 mol%) composition. As in the case of high-temperature mullites, the cause of these structural and compositional variations is not clearly understood.[66,73]

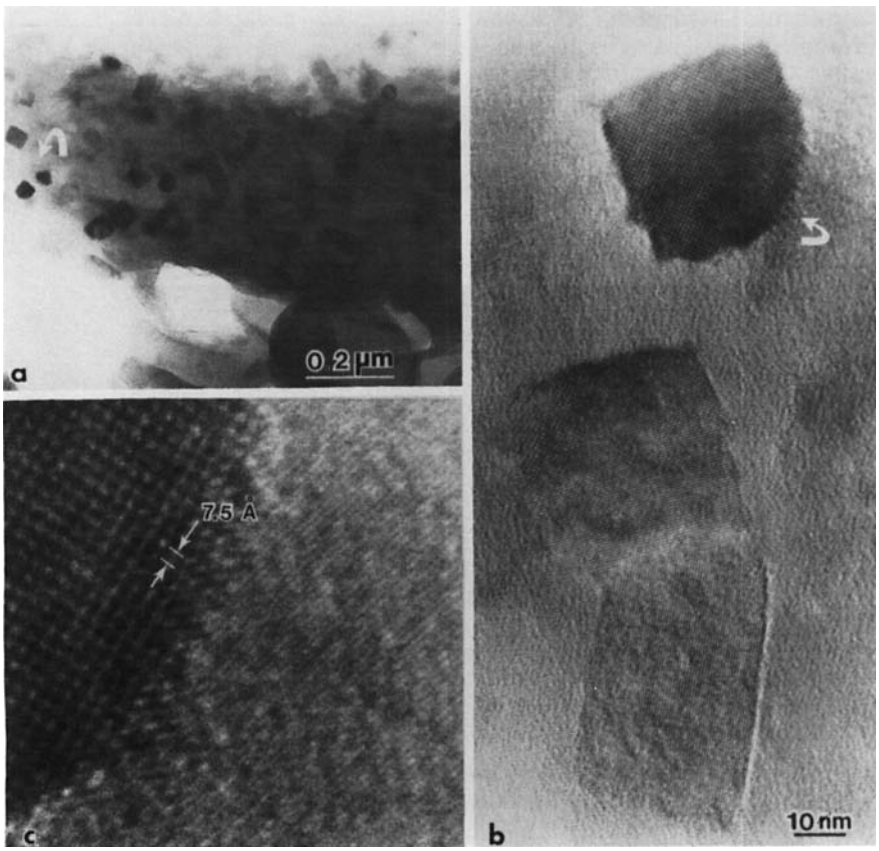

Fig. 9. (A) TEM bright-field image of an alumina–kaolinite sample with an overall composition of mullite after heat treatment at 1300°C for 1 h. Image reveals the formation of nanometer-sized mullite crystallites in an amorphous silica-rich matrix. (B) High-magnification and high-resolution image of two mullite crystallites. (C) Higher magnification image of the region shown by arrow in (B) revealing the interface that is developing between the crystallites.

(3) Low-Temperature (<1350°C) Sintering through Viscous Densification

Although various elegant methods have been developed to produce submicrometer-sized and phase-pure mullite powders, the pressureless sintering of these powders to a fully dense state at temperatures below 1500°C has not been possible (Fig. 7) mainly because of the low interdiffusion rates of silicon and aluminum ions in crystalline mullite.[48,77] To circumvent this problem, the approach that is now preferred for low-temperature (<1350°C) densification is sintering through viscous deformation of amorphous mullite-forming systems prior to total mullitization. Thus, delaying the mullitization step to higher temperatures is an essential requirement for the success of this approach. A study of phase formation during densification shows that, in addition to mullite, the crystallization of cristobalite in the temperature range of 1275° to 1350°C also contributes to retarding densification rates (Fig. 10).[48,59,62] Various methods have been developed to implement densification via viscous phase deformation (Fig. 7).[48,53,54,58,59,62] For instance, with diphasic sol–gel-based systems, nearly fully dense (>98.5%) states have been achieved at temperatures as low as 1250°C.[48,50,54] In recent studies, composite particles of alumina coated with amorphous silica have been used to achieve the same result without the deleterious effects of excessive shrinkage experienced in the sol–gel-based systems during densification.[59,62]

V. Mechanical Properties

Mullite has never been considered suitable for high-strength applications at low temperatures. Depending on the microstructural features, the low fracture toughness of mullite (about 2.2 $MPa \cdot m^{1/2}$) limits its strength to the range of 200 to 500 MPa.[78–84] For high-temperature applications, however, mullite has long been recognized for its excellent resistance to creep and thermal shock in refractories.[84,87] Furthermore, recent studies have shown that phase-pure mullite can also retain its strength to temperatures as high as 1500°C.[78,84] Combined with its intrinsic thermal stability under oxidizing condi-

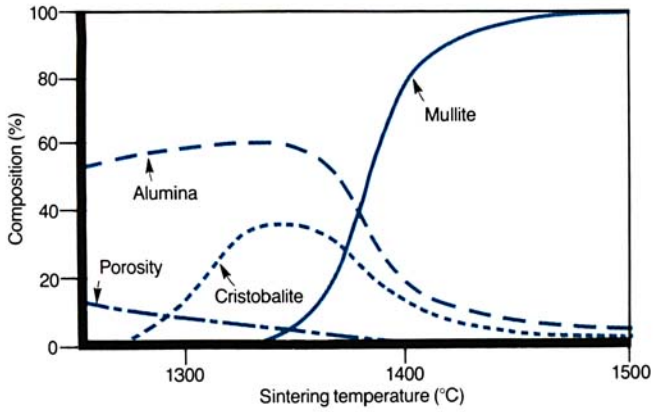

Fig. 10. Evolution of phases in a colloidally consolidated compact of composite powders during viscous-phase sintering.[62] Densification is completed in the temperature range of 1300° to 1400°C. In this range, cristobalite crystallization is dominant. Mullite nucleation and growth starts at ~1350°C and coincides with the dissolution of alumina.

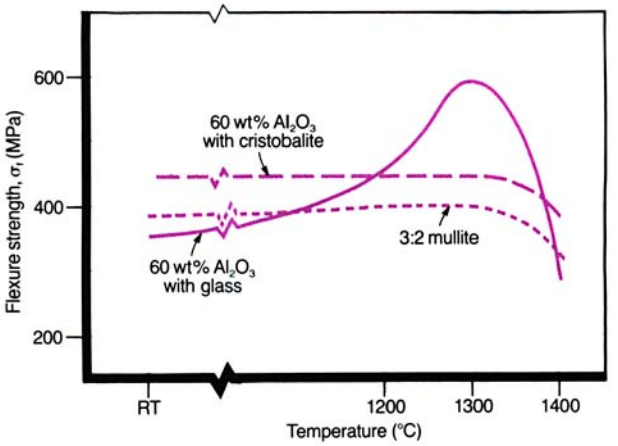

Fig. 11. Flexural strength of mullite and mullite composites as a function of temperature. Phase-pure mullite retains >90% of its strength at 1400°C. Glass-containing mullite, however, starts losing its strength above 1300°C after an initial increase due to the presence of the viscous phase. After the crystallization of this phase to cristobalite, the behavior resembles that of phase-pure mullite.[82,83]

tions, mullite then stands out as a unique material for high-temperature applications not only as a single-phase material but also as a matrix material in the development of high-temperature composites. Consequently, over the last decade, research work has concentrated on two key areas: (i) understanding the role of microstructural features that affect high-temperature strength and creep resistance[4,79–84,87] and (ii) increasing the fracture toughness of mullite through composite engineering.[2,88–91]

(1) High-Temperature Strength

In the polycrystalline form, the most essential requirement for retaining the strength of mullite at elevated temperatures appears to be the elimination of glassy boundaries. As illustrated in Fig. 11, when a polycrystalline mullite is not phase pure, although a noticeable increase in strength occurs above the softening temperature of the glassy inclusions, the effect of the glassy pockets is also to reduce the strength at higher temperatures.[79,82–84] This initial increase in strength corresponds to a similar increase in fracture toughness caused by the blunting of the cracks with the viscous phase.[82,83] Since the softening temperature of siliceous inclusions is expected to increase with the purity level, the maximum in the high-temperature strength shifts to temperatures as high as 1300°C in highly pure systems and can drop below 1000°C as the impurity level increases.[92] When the glassy phase is crystallized to form cristobalite, the maximum in strength disappears, but the resulting mullite–cristobalite composite now retains a higher level of its strength up to 1400°C (Fig. 11).[83] In the absence of glassy inclusions, however, polycrystalline mullite retains a significant portion of its room-temperature strength up to 1500°C.[16,78,83]

(2) Creep Resistance

Significant differences are observed in the creep behavior of phase-pure polycrystalline mullite in comparison to mullite-matrix composites. The first definitive study attesting to the unusually high creep resistance of mullite at 1500°C indicates that mullite in single-crystalline form shows no plastic deformation at stress levels up to 900 MPa (the limit of the instrumental system used).[16] Similarly impressive results have been obtained with polycrystalline mullite without an amorphous boundary phase (Fig. 12).[4] In the case of mullite matrix composites and/or mullites that contain an amorphous boundary phase, creep resistance decreases (Fig. 12).[4] However, when an amorphous boundary phase is present, the steady-state creep resistance is decreased by 2 orders of magnitude when tested under constant stress in the temperature range of 1177° to 1427°C and at stress levels of 5 to 220 MPa. A 20 vol% silicon carbide-whisker-reinforced mullite composite also containing an amorphous phase shows similar behavior, but only 1 order of magnitude decrease in the creep resistance. The three different activation energy regimes also appear to be related to the change in the viscosity of the amorphous phase with temperature.[4] In the middle-temperature regime, cavitation primarily at the grain boundaries appears to be responsible for the high-activation-energy creep, whereas in the low- and high-temperature regimes, cavitation is not observed.

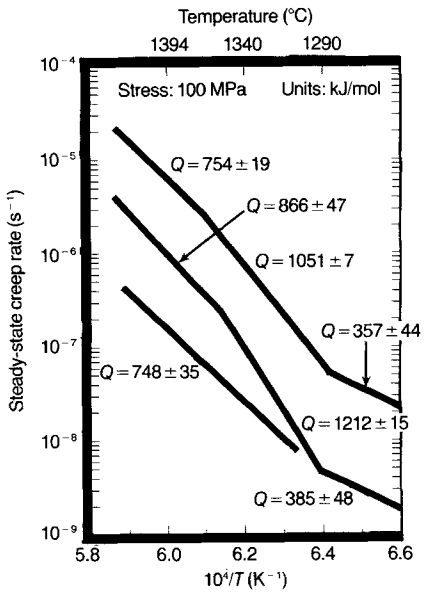

Fig. 12. Steady-state creep rate of mullite and mullite-matrix composites in the temperature range of 1230° to 1430°C at a constant stress of 100 MPa. Upper curve is for a mullite with glassy inclusions and the lower one is for a phase-pure mullite. Middle curve corresponds to a 20 vol% silicon carbide-whisker-reinforced mullite with the composite of mullite + glass of the upper curve used as the matrix.[4]

VI. Electronic Properties

High-performance packaging requirements for new-generation computer systems place a premium on the development of ceramic substrates with a low dielectric constant, high wiring density, and low sintering temperatures to achieve cosintering with metals such as copper and thermal-expansion match to silicon.[5] As a substrate, mullite, with a dielectric constant, $\varepsilon=6.7$, results in about 17% lower signal transmission delay time than alumina ($\varepsilon=9.8$).[5,93] Furthermore, mullite has a low-thermal-expansion coefficient (4×10^{-6}/°C in the 20° to 200°C range), which is almost that of silicon. Consequently, mullite and mullite-based glass-ceramics have now emerged as candidates in high-performance packaging applications.[93,94] As illustrated in Fig. 13, Hitachi's multilayer ceramic system is now totally based on a mullite substrate.[5]

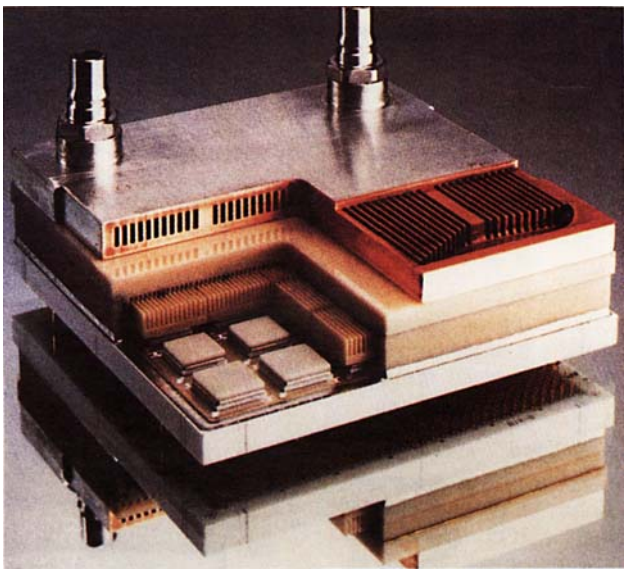

Fig. 13. Mullite-based multilayer electronic package (courtesy of Hitachi).[5]

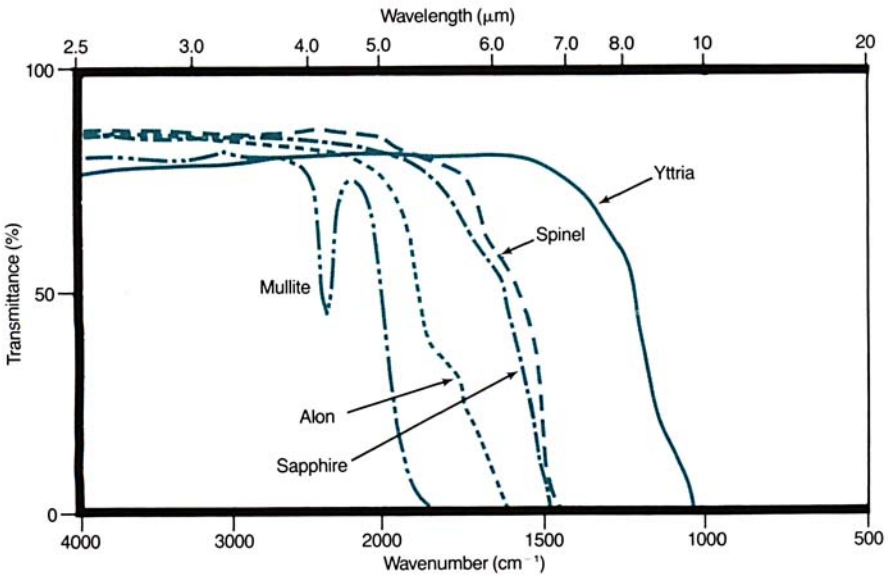

Fig. 14. In-line transmission spectra for monolithic ceramic materials in the mid-infrared ($4000\leq\tilde{\nu}\leq400$ cm^{-1}). ("Alon" is an abbreviation for aluminum oxynitride.) Mullite has a higher cutoff, at $\lambda\approx5$ μm, but the presence of a strong absorbance band at 4.3 μm further reduces its effectiveness as an infrared window. This absorbance has been shown to be related to the process method used and may be caused by the presence of nanometer-sized inhomogeneities in the mullite matrix (Fig. 16). Molecular-scale processing eliminates the 4.3-μm absorption band and improves the utility of mullite as a window material.

Recent research has shown that further reductions in the dielectric constant to values as low as 4.5 can be achieved with a mullite–glass composite.[93] As illustrated in Section IV, with sol–gel or composite powder methods, pure mullite can now be sintered at temperatures as low as 1250°C. Thus, it is quite likely that further reductions in sintering temperatures can be achieved with a mullite–glass composite, thus making mullite an ideal candidate for cosintering with copper.

VII. Optical Properties

Recent interest in the optical properties of mullite has focused on its applicability as a window material within the mid-infrared portion of the spectrum, from 3- to 5-μm wavelength.[95,96] Although various attempts have been made to produce optical-grade mullite[44,45,97] and the infrared characteristics of mullite have been studied extensively since the 1950s,[98–101] the first successful demonstration of mullite as an infrared transparent window by Prochazka and Klug[6] is quite recent. In Fig. 14, we compare the transmissivity of their mullite with various other ceramic materials in this mid-infrared range.[6,95,96] Figure 14 shows that the optical properties of mullite compare favorably to other advanced materials as a potential window material. Two features are of significance: (i) the presence of the 4.3-μm absorption band in the transmittance spectrum of mullite is quite deleterious to the overall properties of the mullite, and (ii) the 5-μm cutoff of mullite windows is below the cutoff of other window materials. As discussed below, the 4.3-μm absorption appears to be associated with processing-related defects and thus may be eliminated, but the 5-μm cutoff is intrinsic to the structure of mullite.

The very large absorption band centered at 4.3 μm was first attributed by Prochazka and Klug[6] to tetrahedral silicon within the mullite matrix (Fig. 14). Subsequent studies illustrated that this band is absent in mullites prepared with CVD-processed powders and monophasic polymeric precursors but is still present in systems processed with diphasic gels (Fig. 15).[48,53,102] A close examination of the sol–gel-processed mullite showed nanometer-sized amorphous inclusions within the mullite

grains, which may be responsible for the 4.3-μm absorption (Fig. 16).

Detailed analysis of mullite grains from densified samples revealed that each grain included isolated, roughly spherical pockets with sizes ranging from 3 to 20 nm. The HREM image presented in Fig. 16 shows such a region in a single grain of mullite in the [010] projection of the lattice. The structure of the amorphous phase in the pockets is discernible from the phase contrast which arises because of the differences in diffraction (crystallinity) and absorption (mass) between the pockets and the mullite matrix. Analysis of the amorphous phase within the pockets was made by electron energy loss spectroscopy, which determined that the phase is composed of about 88 mol% silica and 12 mol% alumina. The presence of pockets with amorphous silica is attributed to the silica, which remains between the AlOOH particles during the gelation step and are then entrapped within the mullite grains during the mullitization process above 1000°C.

The 5-μm cutoff within the infrared range for mullite is due to the Si–O bond within the matrix and is therefore intrinsic to the material. The cutoff region can be shifted for glasses if cations of larger size and lower crystal field strength are used. Thus, germanium oxide has a cutoff at 6 μm, compared to 5 μm for silica.[103] Similarly, in aluminum germanate ($3Al_2O_3 \cdot 2GeO_2$), the germanium analog to mullite, the infrared cutoff shifts to about 6 μm.[104]

The potential applications of infrared-transparent mullite are principally as windows in chemically harsh, hot, or mechanically stressful environments.[95] More recently, mullite glass-ceramics have been studied as a potential matrix material for Cr^{3+}, a luminescent transition metal used as an optical activator in solid-state lasers (see photograph on p. 2349).[105,106] Normally, activators of this type are stabilized and protected by using crystalline "hosts" (e.g., alexandrite) because the electronic structure of the ion is sensitive to the crystal field strength of the crystal. The expense of using crystalline hosts led to an interest in amorphous matrices, but quantum efficiencies for Cr^{3+} were found to fall below 1%.[105] Mullite glass-ceramic was seen as a material of interest because of its stability as a phase, its defect structure, and the low dielectric constant for mullite glass-ceramics. In mullite, Cr^{3+} quantum efficiencies increased by 30% to 40%, and optical gain was found to be almost one-third that of Cr^{3+} in alexan-

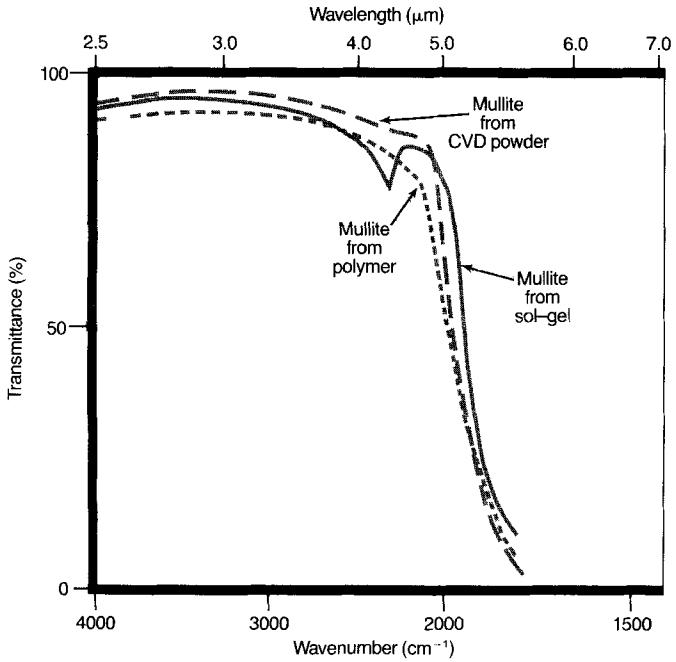

Fig. 15. Optically transparent mullites made using three processes: sol-gel, CVD, and polymeric precursors. Two techniques which use atomic-scale mixing of the alumina- and silica-containing moieties (CVD and polymer) succeed in eliminating the absorption band centered at 4.3 μm observed in the sol-gel-derived material. However, it is possible to reduce or eliminate this band in mullite from carefully prepared sol-gels, indicating that the 4.3-μm band may be used as a quality-control indicator in mullite processing.

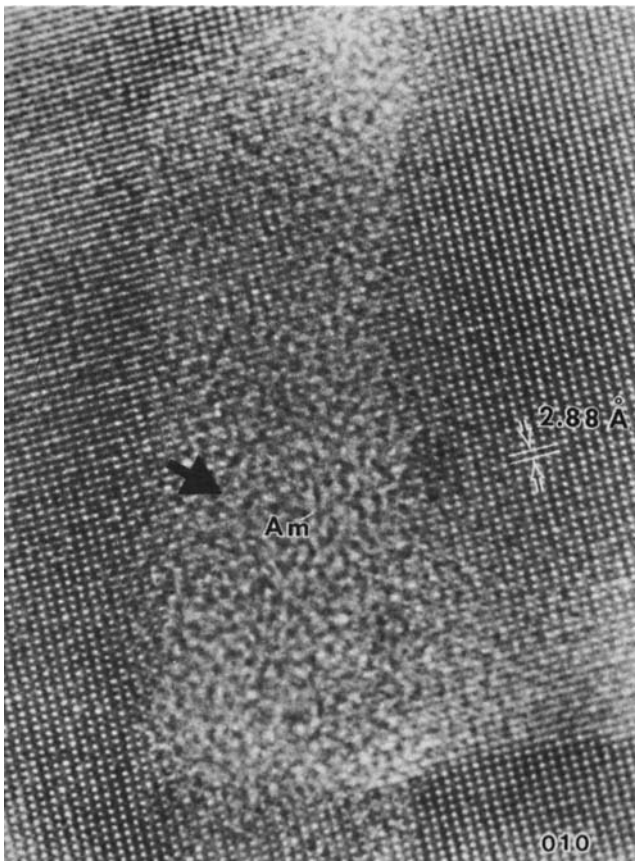

Fig. 16. HREM image of a mullite grain recorded in the [010] projection of the mullite lattice revealing a pocket of amorphous phase engulfed within the grain, as indicated by an arrow. Composition of the pocket is 88 mol% silica and 12 mol% alumina.

drite.[106] Increasing crystallinity in the mullite glass-ceramic reduced scattering losses, indicating that the Cr^{3+} ion preferentially resides in the crystalline phase and that it is possible to synthesize polycrystalline materials approaching the quality of laser crystals.

VIII. Conclusions

The current intense interest in mullite as an important candidate material for demanding structural, electronic, and optical applications is well justified. Its attractive properties include excellent high-temperature strength and resistance to creep and thermal shock, low dielectric and thermal-expansion constants, and good transmission at high temperatures in the mid-infrared band. However, despite the advances in fundamental research on mullite in recent years, much more laboratory research and development is required before the full potential of mullite, as an advanced ceramic material, can be realized.

After decades of controversy, uncertainties about the phase equilibria of the silica–alumina system still continue. Conflicting views mainly arise when only *one* method of analysis is used to determine the phase diagram. More properly, in addition to microstructural characterization, the overall composition must also be profiled to determine the stable and metastable equilibrium conditions. On this basis, the phase diagram shown in Fig. 2(A) is the most unifying one since it combines the results of various methods to provide an overall view for all stable and metastable states.

Large variations in the composition of mullite, ranging from $3Al_2O_3 \cdot 2SiO_2$ to $3Al_2O_3 \cdot SiO_2$, appear to relate to the defect structure as manifested by the ordering/disordering of oxygen vacancies. Additional studies are needed to determine the limits of sub-phase fields for mullites of different compositions. Controversy still attends the nature of the ordered and disordered structures which appear in mullites prepared under different conditions. Although it is probable that several different forms of mullite exist in a given sample, much more work is needed to clarify these structures and their effect upon phase stabilities and physical properties.

Almost single-phase mullite can now be produced at temperatures between 1250° and 1500°C using molecular and/or colloidal mullite precursors. Precursors with atomic-scale homogeneity convert directly to mullite at temperatures near 980°C, but these precursors are not ideal for the low-temperature sintering of mullite. In contrast, with diphasic precursors (with a scale of homogeneity from 1 to 100 nm) and silica-coated particles, mullite formation is delayed to the 1300° to 1550°C range, and, thus, these systems provide the means for low-temperature sintering via viscous deformation. However, although viscous sintering is beneficial, especially in the processing of composites, it is essential that glassy inclusions must later be converted to crystalline phases since glass-free grain boundaries are prerequisite to maintaining the high-temperature strength of mullite and to maintaining high creep resistance.

Mullite is a suitable electronic packaging material because of its low dielectric constant and thermal-expansion coefficient. Lower dielectric constants can be achieved using glass-ceramics, and this has led to possible applications of mullite in solid-state lasers. Similarly, as a material of interest for windows in the mid-infrared spectrum, mullite is especially suited for high-temperature applications. A deleterious absorption band centered at 4.3 μm appears to be connected with the presence of small amorphous inclusions within the grains; this band can be eliminated through careful processing or the use of monophasic precursors.

Acknowledgments: R.F. Davis, R.M. Fisher, G.L. Messing, J.A. Pask, and M.D. Sacks provided a critical review of the manuscript, and their efforts are much appreciated. The courtesy of E.A. Richards (3M Company) in providing Fig. 8, of the Hitachi Corporation in providing Fig. 13, and of G.H. Beall (Corning, Inc.) in providing Fig. 17 is similarly appreciated. The assistance of M.S. Wallace and C. Reeder in the preparation of the manuscript is gratefully acknowledged.

References

[1]F.H. Norton, *Fine Ceramics, Technology, and Applications;* pp. 1–91. McGraw-Hill, New York, 1970.

[2]P.F. Becher, "Microstructural Design of Toughened Ceramics," *J. Am. Ceram. Soc.*, **74** [2] 255–69 (1991).

[3]S. Sōmiya and Y. Hirata, "Mullite Powder Technology and Applications in Japan," *Am. Ceram. Soc. Bull.*, **70** [10] 1624–32 (1991).

[4]R.D. Nixon, S. Chevacharoenkul, R.F. Davis, and T.N. Tiegs, "Creep of Hot-Pressed SiC-Whisker-Reinforced Mulliite"; pp. 579–603 in Ceramic Transactions, Vol. 6, *Mullite and Mullite Matrix Composites.* Edited by S. Sōmiya, R.F. Davis, and J.A. Pask. American Ceramic Society, Westerville, OH, 1990.

[5]R.R. Tummala, "Ceramic and Glass-Ceramic Packaging in the 1990s," *J. Am. Ceram. Soc.*, **74** [5] 895–908 (1991).

[6]S. Prochazka and F.J. Klug, "Infrared-Transparent Mullite Ceramic," *J. Am. Ceram. Soc.*, **66** [12] 874–80 (1983).

[7]N.L. Bowen and J.W. Greig, "The System: Al_2O_3–SiO_2," *J. Am. Ceram. Soc.*, **7** [4] 238–54 (1924); *ibid.*, p. 410.

[8]E.S. Shepard, G.A. Rankin, and W. Wright, "The Binary Systems of Alumina and Silica, Lime and Magnesia," *Am. J. Sci.*, **28** [166] 293–333 (1909).

[9]J.L. Holm and O.J. Kleppa, "The Thermody-

namic Properties of the Aluminum Silicates," *Am. Mineral.*, **51** [11–12] 1608–22 (1966).

[10]G. S. Johnstone and W. Mykura, *The Northern Highlands of Scotland,* 4th ed; pp. 138–43. British Geological Survey, HM's Stationery Office, London, U.K., 1989.

[11]N. L. Bowen, J. W. Greig, and E. G. Zies, "Mullite, a Silicate of Alumina," *J. Wash. Acad. Sci.*, **14** [9] 183–91 (1924).

[12]J. Grofcsik and F. Tamas, *Mullite, Its Structure, Formation, and Significance.* Publishing House of the Hungarian Academy of Sciences, Budapest, Hungary, 1961.

[13]W. H. Bauer, I. Gordon, and C. H. Moore, "Flame Fusion Synthesis of Mullite Single Crystals," *J. Am. Ceram. Soc.*, **33** [4] 140–43 (1950).

[14]W. H. Bauer and I. Gordon, "Flame Fusion Synthesis of Several Types of Silicate Structures," *J. Am. Ceram. Soc.*, **34** [8] 250–54 (1951).

[15]R. F. Davis and J. A. Pask, "Mullite"; pp. 37–76 in *High-Temperature Oxides,* Part IV. Edited by A. M. Alper. Academic Press, New York, 1971.

[16]P. C. Dokko, J. A. Pask, and K. S. Mazdiyasni, "High-Temperature Mechanical Properties of Mullite Under Compression," *J. Am. Ceram. Soc.*, **60** [3–4] 150–55 (1977).

[17]Ceramic Transactions, Vol. 6, *Mullite and Mullite Matrix Composites.* Edited by S. Sōmiya, R. F. Davis, and J. A. Pask. American Ceramic Society, Westerville, OH, 1990.

[18]"Symposium F: Mullite Processing, Structrure, and Properties" (American Ceramic Society Pacific Coast Regional Meeting), *Am. Ceram. Soc. Bull.*, **69** [9] 1526–27 (1990).

[19]S. Aramaki and R. Roy, "Revised Phase Diagram for the System Al_2O_3–SiO_2," *J. Am. Ceram. Soc.*, **45** [5] 229–42 (1962).

[20]I. A. Aksay and J. A. Pask, "The Silica–Alumina System: Stable and Metastable Equilibria at 1.0 Atmosphere," *Science (Washington, D.C.),* **183** [4120] 69–71 (1974).

[21]I. A. Aksay, and J. A. Pask, "Stable and Metastable Equilibria in the System SiO_2–Al_2O_3," *J. Am. Ceram. Soc.*, **58** [11–12] 507–12 (1975).

[22]F. J. Klug, S. Prochazka, and R. H. Doremus, "Al_2O_3–SiO_2 System in the Mullite Region," *J. Am. Ceram. Soc.*, **70** [10] 750–59 (1987).

[23]F. J. Klug, S. Prochazka, and R. H. Doremus, "Alumina–Silica Phase Diagram in the Mullite Region"; pp. 15–43 in Ceramic Transactions, Vol. 6, *Mullite and Mullite Matrix Composites.* Edited by S. Sōmiya, R. F. Davis, and J. A. Pask, American Ceramic Society, Westerville, OH, 1990.

[24]J. A. Pask, "Critical Review of Phase Equilibria in the Al_2O_3–SiO_2 System"; pp. 1–13 in Ceramic Transactions, Vol. 6, *Mullite and Mullite Matrix Composites.* Edited by S. Sōmiya, R. F. Davis, and J. A. Pask. American Ceramic Society, Westerville, OH, 1990.

[25]R. Roy, "The Al_2O_3–SiO_2 Phase Diagram: Metastability and Order–Disorder"; pp. 45–50 in Ceramic Transactions, Vol. 6, *Mullite and Mullite Matrix Composites.* Edited by S. Sōmiya, R. F. Davis, and J. A. Pask. American Ceramic Society, Westerville, OH, 1990.

[26]S. H. Risbud, "Revisiting Metastable Immiscibility and Structure in Silica–Alumina Glasses"; pp. 61–71 in Ceramic Transactions, Vol. 6, *Mullite and Mullite Matrix Composites.* Edited by S. Sōmiya, R. F. Davis, and J. A. Pask. American Ceramic Society, Westerville, OH, 1990.

[27]J. A. Pask and I. A. Aksay, "Determination of Phase Diagrams Using Diffusion Techniques"; pp. 433–44 in *Mass Transport Phenomena in Ceramics,* Materials Science Research, Vol. 9. Edited by A. R. Cooper and A. H. Heuer. Plenum Press, New York, 1975.

[28]D. G. W. Smith and J. D. C. McConnel, "A Comparative Electron Diffraction Study of Sillimanite and Some Natural and Artificial Mullites," *Mineral. Mag.*, **35** [274] 810–14 (1966).

[29](a) R. W. G. Wyckoff, J. W. Greig, and N. L. Bowen, "The X-ray Diffraction Pattern of Mullite and Sillimanite," *Am. J. Sci.*, **11**, 459–72 (1926). (b) W. H. Taylor, "The Structure of Sillimanite and Mullite," *Z. Kristallogr.*, **68**, 503–21 (1928).

[30]S. O. Agrell and J. V. Smith, "Cell Dimensions, Solid Solution, Polymorphism, and Identification of Mullite and Sillimanite," *J. Am. Ceram. Soc.*, **43** [2] 69–76 (1960).

[31]R. Sadanaga, M. Tokonami, and Y. Takaeuchi, "The Structure of Mullite: $2Al_2O_3 \cdot SiO_2$, and Relationship with the Structure of Sillimanite and Andalusite," *Acta Crystallogr.*, **15**, 65–68 (1962).

[32]W. E. Cameron, "Compositions and Cell Dimensions in Mullite," *Am. Ceram. Soc. Bull.*, **56** [11] 1003–11 (1977).

[33]W. E. Cameron, "Mullite: A Substituted Alumina," *Am. Mineral.*, **62** [7–8] 747–55 (1977).

[34]H. Saalfeld, "The Domain Structure of 2:1 Mullite ($2Al_2O_3 \cdot SiO_2$)," *Mineral. Abh.*, **134** [3] 305–16 (1979).

[35]C. W. Burnham, "Compositional Limits of Mullite and the Sillimanite–Mullite Solid Solution Problem," *Carnegie Inst. Washington, Year Book,* **63**, 227–29 (1964).

[36]Y. Nakajima, N. Morimoto, and E. Watanabe, "Direct Observation of Oxygen Vacancy in Mullite, $1.86Al_2O_3 \cdot SiO_2$ by High-Resolution Electron Microscopy," *Proc. Jpn. Acad.*, **51** [3] 173–78 (1975).

[37]R. J. Angel and C. T. Prewitt, "Crystal Structure of Mullite: A Reexamination of the Average Structure," *Am. Mineral.*, **71**, 1476–82 (1986).

[38]S. Durovic, "Refinement of the Crystal Structure of Mullite," *Slovak. Acad. Sci., Cheicke Zvesti,* **23** [2] 113–28 (1969).

[39]M. Tokonami, Y. Nakajima, and N. Morimoto, "The Diffraction Aspect and a Structural Model of Mullite, $Al(Al_{1+2x}Si_{1-2x})O_{5-x}$," *Acta Crystallogr., Sect. A: Cryst. Phys., Diffr., Theor. Gen. Crystallogr.*, **36** [2] 270–76 (1980).

[40]J. D. C. McConnel and V. Heine "Incommensurate Structure and Stability of Mullite," *Phys. Rev. B: Condens. Matter,* **31**, 6140–42 (1985).

[41]W. M. Kriven and J. A. Pask, "Solid-Solution Range and Microstructure of Melt-Grown Mullite," *J. Am. Ceram. Soc.*, **66** [9] 649–54 (1983).

[42]Y. Nakajima and P. H. Ribbe, "Twinning and Superstructure of Al-Rich Mullite," *Am. Mineral.*, **66**, 142–47 (1981).

[43]T. Epicier, M. A. O'Keefe, and G. Thomas, "Atomic Imaging of 3:2 Mullite," *Acta Crystallogr., Sect. A: Cryst. Phys., Diffr., Theor. Gen. Crystallogr.*, **46**, 948–62 (1990).

[44]K. S. Mazdiyasni and L. M. Brown, "Synthesis and Mechanical Properties of Stoichiometric Aluminum Silicate (Mullite)," *J. Am. Ceram. Soc.*, **55** [11] 548–52 (1972).

[45]B. E. Yoldas, "Microstructure of Monolithic Materials Formed by Heat Treatment of Chemically Polymerized Precursors in the SiO_2–Al_2O_3 Binary," *Am. Ceram. Soc. Bull.*, **59** [4] 479–83 (1980).

[46]D. W. Hoffman, R. Roy, and S. Komarneni, "Diphasic Xerogels, A New Class of Materials: Phases in the System Al_2O_3–SiO_2," *J. Am. Ceram. Soc.*, **67** [7] 468–71 (1984).

[47]P. D. D. Rodrigo and P. Boch, "High-Purity Mullite Ceramics by Reaction Sintering," *Int. J. High Technol. Ceram.*, **1**, 3–30 (1985).

[48]N. Shinohara, D. M. Dabbs, and I. A. Aksay, "Infrared Transparent Mullite through Densification of Monolithic Gels at 1250°C"; *Infrared Opt. Transm. Mater., Proc. SPIE,* **683**, 19–24 (1986).

[49]T. Kumazawa, S. Kanzaki, J. Asaumi, O. Abe, and H. Tabata, "Sinterability of SiO_2–Al_2O_3 Prepared by Spray Pyrolysis: Effect of Chemical Composition," *Yogyo Kyokaishi,* **94** [5] 485–90 (1986).

[50]S. Komarneni, Y. Suwa, and R. Roy, "Application of Compositionally Diphasic Xerogels for En-

hanced Densification: The System Al_2O_3–SiO_2," *J. Am. Ceram. Soc.*, **69** [7] C-155–C-156 (1986).

[51]H. Suzuki and H. Saito, "Processing of the Fine Mullite Powder from Metal Alkoxides and Its Sintering," *Yogyo Kyokaishi*, **95** [7] 697–702 (1987).

[52]J. A. Pask, X.W. Zhang, A.P. Tomsia, and B.E. Yoldas, "Effect of Sol–Gel Mixing on Mullite Microstructure and Phase Equilibria in the α-Al_2O_3–SiO_2 System," *J. Am. Ceram. Soc.*, **70** [10] 704–707 (1987).

[53]Y. Hirata and I. A. Aksay, "Colloidal Consolidation and Sintering Behavior of CVD-Processed Mullite Powders"; pp. 611–21 in *Ceramic Microstructures '86: Role of Interfaces*, Materials Science Research, Vol. 21. Edited by J. A. Pask and A. G. Evans. Plenum Press, New York, 1987.

[54]B. Sonuparlak, "Sol–Gel Processing of Infrared Transparent Mullite," *Adv. Ceram. Mater.*, **3** [3] 263–67 (1988).

[55]W. C. Wei and J.W. Halloran, "Phase Transformation of Diphasic Aluminosilicate Gels," *J. Am. Ceram. Soc.*, **71** [3] 166–72 (1988).

[56]W. C. Wei and J.W. Halloran, "Transformation Kinetics of Diphasic Aluminosilicate Gels," *J. Am. Ceram. Soc.*, **71** [7] 581–87 (1988).

[57]J. C. Huling and G. L. Messing, "Hybrid Gels for Homoepitactic Nucleation of Mullite," *J. Am. Ceram. Soc.*, **72** [9] 1725–29 (1989).

[58]Y. Hirata, I. A. Aksay, R. Kurita, S. Hori, and H. Kaji, "Processing of Mullite with Powders Processed by Chemical Vapor Deposition"; pp. 323–38 in Ceramic Transactions, Vol. 6, *Mullite and Mullite Matrix Composites*. Edited by S. Sōmiya, R. F. Davis, and J. A. Pask. American Ceramic Society, Westerville, OH, 1990.

[59]M. D. Sacks, N. Bozkurt, and G.W. Scheiffele, "Fabrication of Mullite and Mullite-Matrix Composites by Transient Viscous Sintering of Composite Powders," *J. Am. Ceram. Soc.*, **74** [10] 2428–37 (1991).

[60]J. C. Huling and G. L. Messing, "Epitactic Nucleation of Spinel in Aluminosilicate Gels and Its Effect on Mullite Crystallization," *J. Am. Ceram. Soc.*, **74** [10] 2374–81 (1991).

[61]S. Wu and N. E. Clausen, "Fabrication and Properties of Low-Shrinkage Reaction-Bonded Mullite," *J. Am. Ceram. Soc.*, **74** [10] 2460–63 (1991).

[62]J. E. Webb, "Processing of Mullite for Use as a Ceramic–Ceramic Composite Matrix Material"; M.S. Thesis. University of Washington, Seattle, WA, Aug. 1991.

[63]E. A. Richards, C. J. Goodbrake, and H. G. Sowman, "Reactions and Microstructure Development in Mullite Fibers," *J. Am. Ceram. Soc.*, **74** [10] 2404–409 (1991).

[64]M. D. Sacks, H.-W. Lee, and J. A. Pask, "A Review of Powder Preparation Methods and Densification Procedures for Fabricating High-Density Mullite"; pp. 167–207 in Ceramic Transactions, Vol. 6, *Mullite and Mullite Matrix Composites*. Edited by S. Sōmiya, R. F. Davis, and J. A. Pask. American Ceramic Society, Westerville, OH, 1990.

[65]G. W. Brindley and M. Nakahira, "The Kaolinite–Mullite Reaction Series: I–III," *J. Am. Ceram. Soc.*, **42** [7] 311–24 (1959).

[66]K. Okada and N. Otsuka, "Formation Process of Mullite"; pp. 375–87 in Ceramic Transactions, Vol. 6, *Mullite and Mullite Matrix Composites*. Edited by S. Sōmiya, R. F. Davis, and J. A. Pask. American Ceramic Society, Westerville, OH, 1990.

[67]K. Okada and N. Otsuka, "Characterization of the Spinel Phase from SiO_2–Al_2O_3 Xerogels and the Formation Process of Mullite," *J. Am. Ceram. Soc.*, **69** [9] 652–56 (1986).

[68]B. Sonuparlak, M. Sarikaya, and I. A. Aksay, "Spinel Phase Formation at the 980°C Exothermic Reaction in the Kaolinite to Mullite Reaction Series," *J. Am. Ceram. Soc.*, **70** [11] 837–42 (1987).

[69]J. A. Pask and A. P. Tomsia, "Formation of Mullite From Sol–Gel and Kaolinite," *J. Am. Ceram. Soc.*, **74** [10] 2367–73 (1991).

[70]S. Hori and R. Kurita, "Characterization and Sintering of Al_2O_3–SiO_2 Powders Formed by *Chemical Vapor Deposition*"; pp. 311–22 in Ceramic Transactions, Vol. 6, *Mullite and Mullite Matrix Composites*. Edited by S. Sōmiya, R. F. Davis, and J. A. Pask. American Ceramic Society, Westerville, OH, 1990.

[71]T. Kumazawa and S. Ohta, "Influence of Powder Characteristics on Microstructure and Mechanical Properties of Mullite Ceramics"; pp. 401–11 in Ceramic Transactions, Vol. 6, *Mullite and Mullite Matrix Composites*. Edited by S. Sōmiya, R. F. Davis, and J. A. Pask. American Ceramic Society, Westerville, OH, 1990.

[72]Y. Hirata, H. Minamuzono, and K. Shimada, "Property of SiO_2–Al_2O_3 Powders Prepared from *Metal Alkoxides*," *Yogyo Kyokaishi*, **93** [1] 46–54 (1985).

[73]K. Okada and N. Otsuka, "Change in Chemical Composition of Mullite Formed from $2SiO_2 \cdot 3Al_2O_3$ Xerogel During the Formation Process," *J. Am. Ceram. Soc.*, **70** [10] C-245–C-247 (1987).

[74]S. Sundaresan and I. A. Aksay, "Mullitization of Diphasic Aluminosilicate Gels," *J. Am. Ceram. Soc.*, **74** [10] 2388–92 (1991).

[75]M. Sarikaya, I. A. Aksay, and G. Thomas, "High-Resolution Electron Microscopic Characterization of Interfaces of Ceramics"; pp. 167–78 in *Advances in Materials Characterization-II*. Edited by R. L. Snyder, R. A. Condrate, Sr., and P. F. Johnson. Plenum Press, New York, 1985.

[76]J. Ossaka, "Tetragonal Mullite-like Phase from Coprecipitated Gels," *Nature (London)*, **191** [4792] 1000–1001 (1961).

[77]I. A. Aksay, "Diffusion and Phase Relationship Studies in the Alumina–Silica System"; Ph.D. Thesis. University of California, Berkeley, CA, April 1973; Rept. No. UCLBL-1403.

[78]T.-I. Mah and K. S. Mazdiyasni, "Mechanical Properties of Mullite," *J. Am. Ceram. Soc.*, **66** [10] 699–703 (1983).

[79]S. Kanzaki, H. Tabata, T. Kumazawa, and S. Ohta, "Sintering and Mechanical Properties of Stoichiometric Mullite," *J. Am. Ceram. Soc.*, **68** [1] C-6–C-7 (1985).

[80]M. G. M. U. Ismail, Z. Nakai, and K. Minegishi, "Synthesis of Mullite Powder and Its Characteristics," *Int. J. High Technol. Ceram.*, **2** [2] 123–34 (1986).

[81]M. G. M. U. Ismail, Z. Nakai, and S. Sōmiya, "Microstructure and Mechanical Properties of Mullite Prepared by the Sol–Gel Method," *J. Am. Ceram. Soc.*, **70** [1] C-7–C-8 (1987).

[82]T. Kumazawa, S. Kanzaki, S. Ohta, and H. Tabata, "Influence of Chemical Composition on the Mechanical Properties of SiO_2–Al_2O_3 Ceramics," *Yogyo-Kyokaishi*, **96** [1] 85–91 (1988).

[83]T. Kumazawa, S. Ohta, S. Kanzaki, and Z. Nakagawa, "Mechanical Properties of Mullite–Cristobalite Composite"; p. 34 (1B15) in Extended Abstracts of the Annual Meeting, The Ceramic Society of Japan, Tokyo, 1990.

[84]H. Ohnishi, T. Kawanami, A. Nakahira, and K. Niihara, "Microstructure and Mechanical Properties of Mullite Ceramics," *Yogyo Kyokaishi*, **98** [6] 541–47 (1990).

[85]C. O. Hulse and J. A. Pask, "Analysis of Deformation of a Fireclay Refractory," *J. Am. Ceram. Soc.*, **49** [6] 312–18 (1966).

[86]P. A. Lessing, R. S. Gordon, and K. S. Mazdiyasni, "Creep of Polycrystalline Mullite," *J. Am. Ceram. Soc.*, **58** [3–4] 149 (1975).

[87]A. P. Hynes and R. H. Doremus, "High-Temperature Compressive Creep of Polycrystalline Mullite," *J. Am. Ceram. Soc.*, **74** [10] 2469–75 (1991).

[88]N. Claussen and J. Jahn, "Mechanical Properties of Sintered in-situ-Reacted Mullite Zirconia

Composites," *J. Am. Ceram. Soc.*, **63** [3–4] 228–29 (1980).

[89]J. S. Moya and M. I. Osendi, "Microstructure and Mechanical Properties of Mullite/ZrO_2 Composites," *J. Mater. Sci.*, **19** [9] 2909–14 (1984).

[90]P. F. Becher and T. N. Tiegs, "Toughening Behavior Involving Multiple Mechanisms: Whisker Reinforcement and Zirconia Toughening," *J. Am. Ceram. Soc.*, **70** [9] 651–54 (1987).

[91]Y. Hirata, S. Matsushita, Y. Ishihara, and H. Katsuki, "Colloidal Processing and Mechanical Properties of Whisker-Reinforced Mullite-Matrix Composites," *J. Am. Ceram. Soc.*, **74** [10] 2438–42 (1991).

[92]I. Peretz and R. C. Bradt, "Andalusite-Derived Mullite-Matrix Refractories"; pp. 613–33 in Ceramic Transactions, Vol. 6, *Mullite and Mullite Matrix Composites*. Edited by S. Sōmiya, R. F. Davis, and J. A. Pask. American Ceramic Society, Westerville, OH, 1990.

[93]E. A. Giess, J. M. Roldan, P. J. Bailey, and E. Goo, "Microstructure and Dielectric Properties of Mullite Ceramics"; pp. 167–72 in Ceramic Transactions, Vol. 15, *Microelectronic Systems*. Edited by K. M. Nair, R. C. Pohanka, and R. C. Buchanan. American Ceramic Society, Westerville, OH, 1990.

[94]S. Kanzaki, M. Ohashi, H. Tabata, T. Kurihara, S.-I. Iwai, and S.-I. Wakabayashi, "Mullite–Silica Ceramics for Insulating Substrate Material"; pp. 389–99 in Ceramic Transactions, Vol. 6, *Mullite and Mullite Matrix Composites*. Edited by S. Sōmiya, R. F. Davis, and J. A. Pask. American Ceramic Society, Westerville, OH, 1990.

[95]S. Musikant, "Development of a New Family of Improved Infrared (IR) Dome Ceramics," *Emerging Opt. Mater., Proc. SPIE*, **297**, 2–12 (1981).

[96]R. L. Gentilman, "Current and Emerging Materials for 3–5 Micron IR Transmission," *Infrared Opt. Transm. Mater., Proc. SPIE*, **683**, 2–11 (1986).

[97]B. E. Yoldas, "A Transparent Porous Alumina," *Am. Ceram. Soc. Bull.*, **54** [3] 286–88 (1975).

[98]R. Roy and E. E. Francis, "Distinction of Sillimanite from Mullite by Infra-Red Techniques," *Am. Mineral.*, **7**, 725–28 (1953).

[99]A. Muan, "Phase Equilibria at Liquidus Temperatures in the System Iron Oxide–Al_2O_3–SiO_2 in Air Atmosphere," *J. Am. Ceram. Soc.*, **40** [4] 121–33 (1957).

[100]B. L. Metcalfe and J. H. Sant, "The Synthesis, Microstructure, and Physical Properties of High-Purity Mullite," *Trans. Br. Ceram. Soc.*, **74**, 193–201 (1975).

[101]K. J. D. MacKenzie, "An Infra-Red Frequency Shift Method for the Determination of the High-Temperature Phase of Aluminosilicate Minerals," *J. Appl. Chem.*, **19**, 65–67 (1969).

[102]J. J. Lannutti, D. R. Treadwell, D. M. Dabbs, and I. A. Aksay, "Evolution of Mullite from Inorganic Polymers"; unpublished work.

[103]W. H. Dumbaugh, "Infrared Transmitting Germanate Glasses," *Emerging Opt. Mater., Proc. SPIE*, **297**, 80–85 (1981).

[104]S. Prochazka and G. A. Slack, "Preparation and Optical Properties of Polycrystalline Aluminum Germanate"; pp. 245–54 in *Better Ceramics Through Chemistry*, Materials Research Society Symposium Proceedings, Vol. 32. Edited by C. J. Brinker, D. E. Clark, and D. R. Ulrich. Materials Research Society, Pittsburgh, PA, 1984.

[105]L. J. Andrews, G. H. Beall, and A. Lempicki, "Luminescence of Cr^{3+} in Mullite Transparent Glass-Ceramics," *J. Lumin.*, **36**, 65–74 (1986).

[106]A. J. Wojtowicz, W. Meng, A. Lempicki, G. H. Beall, D. W. Hall, and T. C. Chin, "Spectroscopic Characteristics of Chromium-Doped Mullite Glass-Ceramics," *IEEE J. Quantum Electron.*, **24** [6] 1109–13 (1988). □

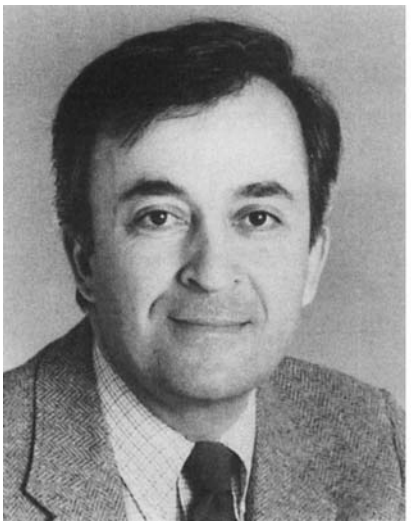

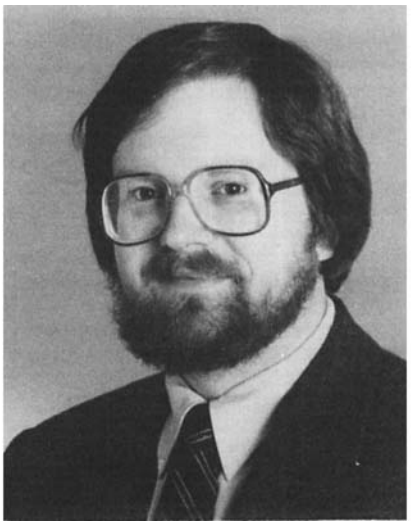

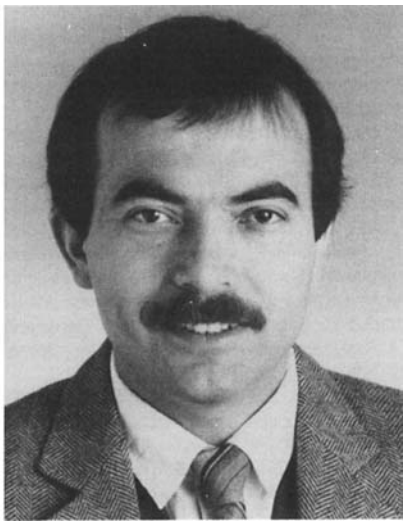

Ilhan A. Aksay is a Professor in the Department of Materials Science and Engineering and the Director of the Advanced Materials Technology Center of the Washington Technology Center at the University of Washington. He earned his B.Sc. degree (with honors) in ceramic engineering at the University of Washington in 1967. He received his M.Sc. degree in 1969 and Ph.D. degree in 1973, both in materials science and engineering at the University of California, Berkeley. Upon completing a one-year postdoctoral appointment at the University of California, Berkeley, he worked at Xerox, Webster Research Center (1973–1975) and the Middle East Technical University in Ankara, Turkey (1975–1981). In 1981, Dr. Aksay joined the Materials Science and Engineering Department at the University of California at Los Angeles as a Visiting Associate Professor. Since 1983, he has been at the University of Washington. His most recent research activities have been on the utilization of colloidal and bioinspired processing techniques in the development of ceramics. In recognition of his contributions in this area, he received the Richard M. Fulrath Award of the American Ceramic Society in 1987. In 1987, he was also named as the first recipient of the Pacific Northwest Laboratory Professorship by the U.S. Department of Energy. He received the 1988 Academic Engineer of the Year Award of the Puget Sound Engineering Council for his "contributions to advances in ceramic processing technology and the transfer of this technology to industry and students." Dr. Aksay is a Fellow of the American Ceramic Society.

Daniel M. Dabbs is a Research Scientist in the Department of Materials Science and Engineering and the Research Manager for the Advanced Ceramic Materials Laboratory of the Washington Technology Center at the University of Washington. He received his B.Sc. degree (1977) in chemistry at Texas Tech University and his M.Sc. degree (1979) in chemistry and Ph.D. degree (1984) in materials science and engineering at the University of Washington. His research interests include the optical properties of ceramic materials and the application of spectroscopy to process control in the fabrication of ceramics from chemical precursors.

Mehmet Sarikaya is an Associate Professor in the Department of Materials Science and Engineering at the University of Washington. He earned his B.Sc. degree in metallurgy at the Middle East Technical University, Ankara, Turkey (1977), and came to the United States with a North Atlantic Treaty Organization scholarship for studies toward his M.Sc. degree (1979) and Ph.D. (1982) degree, which he received in materials science and engineering at the University of California, Berkeley. Prior to joining the University of Washington in 1984, he worked at Lawrence Berkeley Laboratory as a Research Scientist on structural ceramics. His current interests include structure–property relationships in nanocrystalline materials, high-temperature superconductors, cements, and biomimetics, with emphasis on nanostructural interface effects as analyzed by high-resolution transmission electron microscopy techniques.